2018

Void Fraction and Flow Regimes of R134a In Horizontal and Vertical Round Tubes in Developed Adiabatic Conditions

Hongliang Qian
UIUC, United States of America, hqian7@illinois.edu

Predrag S. Hrnjak
pega@illinois.edu

Void Fraction and Flow Regimes of R134a in Horizontal and Vertical Round Tubes in Developed Adiabatic Conditions

Hongliang Qian[1], Pega Hrnjak[1, 2]*

[1] Air Conditioning and Refrigeration Center, University of Illinois at Urbana-Champaign, 1206 West Green Street, Urbana, IL 61801, USA

[2] Creative Thermal Solutions, 2209 Willow Rd., Urbana, IL, USA

* Corresponding author: pega@illinois.edu +1-217-390-5278

ABSTRACT

This paper presents flow regimes and void fraction in horizontal and vertical round tubes ID 7 mm with R134a in the adiabatic conditions and low mass flux (40-150 kg/m^{2}s for horizontal tubes and 65-115 kg/m^{2}s for vertical tubes) captured by a high-speed camera. Horizontal flow patterns are compared to Wojtan-Ursenbacher-Thome flow regime map and some modifications are proposed. Void fraction results for both horizontal and vertical tubes are compared to some widely used correlations. Influences of tube orientation and mass flux on void fraction are discussed. At the same vapor quality condition, void fraction of horizontal tubes is larger than that of vertical tubes. Higher mass flux also results in larger void fraction compared that of lower mass flux.

1. INTRODUCTION

When talking about void fraction in two-phase systems, the term "void" is used for vapor. Even vapor is not emptiness, we will accept that imperfect name. One of more accurate names might be Volumetric Vapor Fraction but our objective here is not to deal with terminology. In a control volume, *volumetric void fraction* is the ratio of the volume of vapor phase over the total volume of the container. By quickly closing valves located at two ends of a test section and recovering the two-phase mixture trapped inside, volumetric void fraction can be determined. Void fraction and its correlations have been studied both theoretically and experimentally during the past several decades. Woldesemayat and Ghajar (2007) compared 68 void fraction correlations for different flow orientations. In addition, Godbole *et al.* (2011) studied 52 correlations on upward vertical two-phase flow. The correlations compared to data in this paper are based on their recommendations. For horizontal flows, Woldesemayat and Ghajar (2007) suggested Rouhani and Axelsson correlation presented in Woldesemayat and Ghajar (2007) as Rouhani I, Armand (1959)-Massena (1960) and the correlation proposed by Woldesemayat and Ghajar (2007). For vertical flows, Woldesemayat and Ghajar (2007) recommended Dix (1971), and two Rouhani and Axelsson correlations presented in Woldesemayat and Ghajar (2007) as Rouhani I and Rouhani II correlations. In addition, Godbole *et al.* (2011) suggested the correlation by Nicklin (1962) as well. For both horizontal and vertical flows, homogeneous correlation is the upper limit of void fraction. Correlations studied in this paper are shown in Table 1.

Two-phase flow pattern maps which have some transition criteria to diagnose different flow regimes in a two-dimensional diagram are designed to predict local flow patterns from given conditions. Horizontal flow patterns in this paper are compared to Wojtan-Ursenbacher-Thome (Wojtan *et al.*, 2005) flow-pattern map. Some modifications based on the visualization results are proposed. However, no flow-pattern maps for vertical upward refrigerant flows with same format as Wojtan-Ursenbacher-Thome (Wojtan *et al.*, 2005) (quality vs. mass flux diagram) had been proposed yet. Further studies can investigate flow patterns for vertical flows in tubes with refrigerant.

Table 1 Correlations studied in this paper

Reference	Correlation	Category and orientation
Homogeneous	$\alpha_H = [1 + (\frac{1-x}{x})(\frac{\rho_V}{\rho_L})]^{-1}$	Slip ratio, S=1 (H/V*)
Armand (1959)-Massena (1960)	$\alpha = (0.833 + 0.167x)\alpha_H$	$K\alpha_H$ (H)
Nicklin (1962)	$\alpha = \frac{U_{SG}}{(C_0 U_M + U_{GM})}$ where $C_0 = 1.2, U_{GM} = 0.35\sqrt{gD}$	Drift flux (V)
Rouhani and Axelsson (Woldesemayat and Ghajar, 2007) Rouhani I Rouhani II	$\alpha = \frac{U_{SG}}{(C_0 U_M + U_{GM})}$ where $U_{GM} = 1.18(g\sigma\frac{\rho_L - \rho_V}{{\rho_L}^2})^{0.25}$ $C_0 = 1 + 0.2(1-x)$ $C_0 = 1 + 0.2(1-x)(gD\frac{{\rho_L}^2}{G^2})^{0.25}$	Drift flux (H/V)
Dix (1971)	$C_0 = \frac{U_{SG}}{U_{SG}+U_{SL}}\left[1 + \left(\frac{U_{SL}}{U_{SG}}\right)^b\right]$, $b = \left(\frac{\rho_V}{\rho_L}\right)^{0.1}$, $U_{GM} = 2.9\left(g\sigma\frac{\rho_L - \rho_V}{{\rho_L}^2}\right)^{0.25}$	Drift flux (V)
Woldesemayat and Ghajar (2007)	$\alpha = U_{SG} / [U_{SG} \cdot \left(1 + \left(U_{SL}/U_{SG}\right)^{(\rho_v/\rho_l)^{0.1}}\right) +$ $2.9 \cdot \left(gravity \cdot D \cdot \sigma \cdot \left(1+\cos(\theta)\right) \cdot \left(\frac{\rho_l - \rho_v}{{\rho_l}^2}\right)\right)^{0.25} \cdot \left(1.22 + 1.22 \cdot sin(\theta)\right)^{P_{atm}/P}]$	Drift flux (H)

*H: horizontal flows; V: vertical flows

2. FACILITY

The schematic drawing of the facility used is shown in Figure 1. Subcooled liquid refrigerant (R134a) is pumped through a mass flow meter with a gear pump into an electric heater where refrigerant is transformed into superheated vapor. Refrigerant is mixed in the mixer and the condition of refrigerant is determined by measuring its pressure and temperature. Then superheated vapor refrigerant flows into a pre-cooler whose secondary fluid is water. Water is cooled by chilled water (7°C). With the energy balance of the water side in pre-cooler, the condition of refrigerant after the pre-cooler is determined. The pressure transducers are Setra 204 and thermocouples are T-type. The test section includes between two quick closing valves (ball valves, manually open and close) and a visualization part. Figure 2 shows the schematic drawings for horizontal and vertical test sections. The visualization part is a piece of schedule 80 clear PVC tube with inner diameter of 7 mm. Before the visualization section, 600 mm (~86 diameters) of the same PVC tube for the horizontal configuration and 170 mm (~25 diameters) for the vertical configuration is utilized to ensure the flow is fully developed. In addition, for the vertical configuration, 460 mm of tube is maintained before the lower quick-closing valve to eliminate liquid pools within the test section. A high-speed camera is used to capture high-speed video of flow regimes with resolution 512x512 and speed of 2200 frames per second. Phantom CV 2.8 from Vision Research Inc. is used to process the video. The PVC pipe and two ball valves are connected by copper tubes whose inner diameter is 7 mm. The length of test section between two quick closing valves is 1500 mm (~214 diameters) for the horizontal configuration and 750 mm (~107 diameters) for the vertical configuration. Longer test section cannot be achieved due to the space limitation. A bypass loop is parallel to the test section. After the refrigerant passes test section, an after-cooler and a sub-cooler cool the refrigerant into subcooled liquid condition, which is fed into the gear pump to finish the loop.

Table 2 lists the experimental conditions and Table 3 lists uncertainties of the instruments.

Table 2 Experimental conditions

Working media	R134a
T_r	33ºC
Test section orientation	Horizontal and vertical
Test section length	Horizontal: 1500 mm (~214 dia.) Vertical: 750 mm (~107 diameters)
Mass flux	Horizontal: 40, 80, 115 and 150 kg/m^{2}s Vertical: 65, 80 and 115 kg/m^{2}s
Quality	0.05-0.9

Table 3 Uncertainties of the instruments

Measurement point	Variable	Instrument	Uncertainty
Refrigerant and water temperature	T_r, T_w	T-type thermocouple	±0.5 K
Absolute pressure in the mixer and after the test section	P	Absolute pressure transducer (Setra 204)	±0.073% FS (±2.5 kPa)
Refrigerant mass flow rate	m_r	Coriolis mass flow meter	±0.1 g/s
Refrigerant weight	M	Scale (calibrated)	±0.1 g

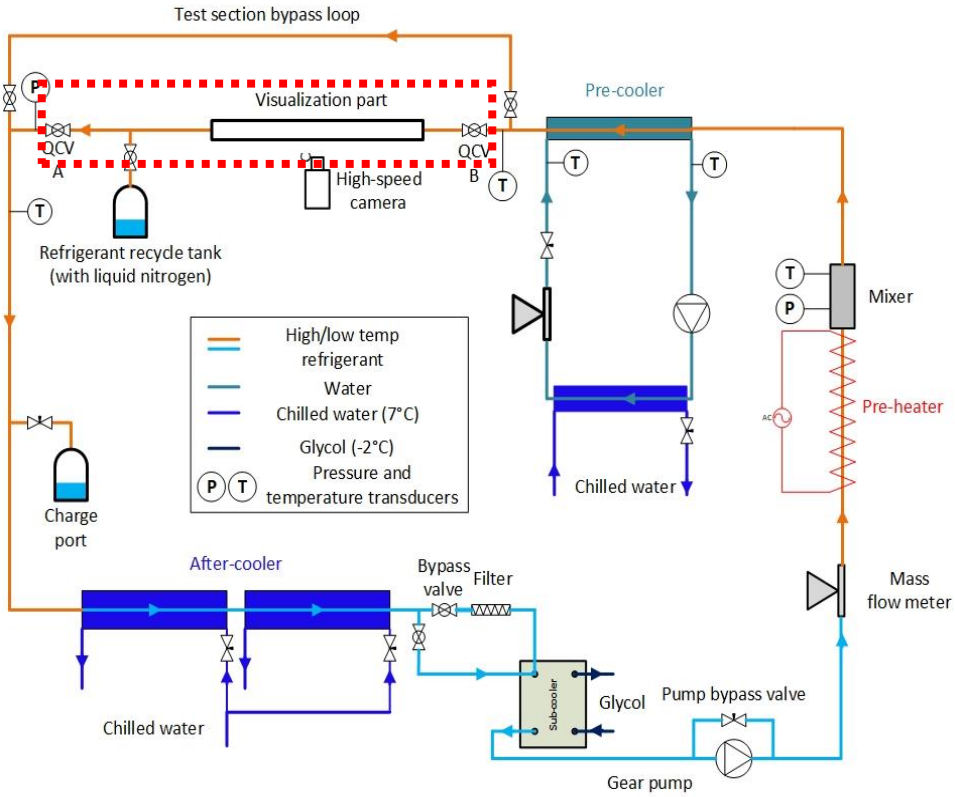

Figure 1 Schematic drawing of experimental facility, test section in the red box

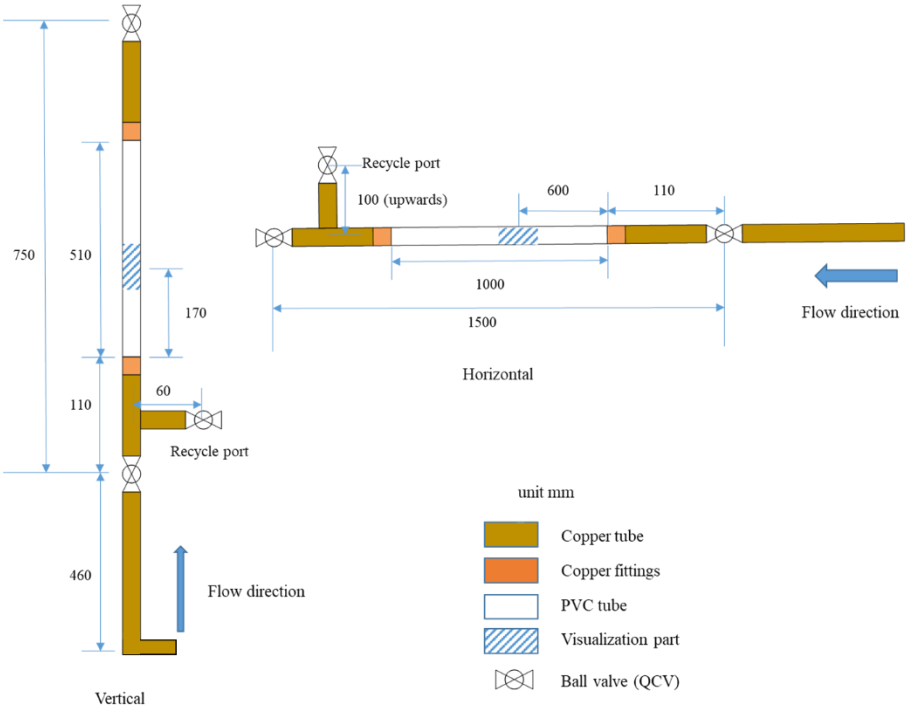

Figure 2 Schematic drawing for horizontal and vertical test section

3. EXPERIMENTAL RESULTS

All data (60 for the horizontal and 60 for the vertical configuration) are presented in Figure 6 and Figure 12.

3.1 Flow regimes and void fraction for horizontal flows

Three major flow regimes: slug/stratified-wavy flow (Figure 3), stratified-wavy flow (Figure 4) and annular flow (Figure 5) are recorded with a high-speed camera, for the horizontal configuration in the mass flux range explored.

Criteria for each flow regime in this paper are listed below:

Slug/stratified-wavy flow: vapor slug appears in the upper portion of the tube periodically with liquid bridges in the middle. Boundary between upper vapor and lower liquid is wavy.

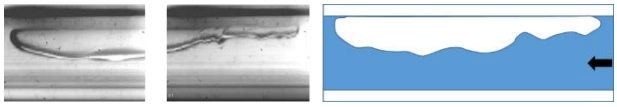

Figure 3 Slug/stratified-wavy flow (R134a, 80 kg/m^{2}s, x=0.1, T=33ºC)

Stratified-wavy flow: liquid flows at the bottom and vapor is in the upper portion of the tube. The interface is wavy, and no liquid bridges fills the entire cross section.

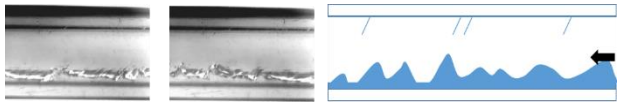

Figure 4 Stratified-way flow (R134a, 115 kg/m^{2}s, x=0.6, T=33ºC)

Annular flow: liquid flows along the tube wall with vapor in the central core. Due to the influence of gravity, the liquid film is thicker at the bottom.

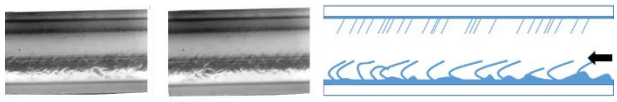

Figure 5 Annular flow (R134a, 150 kg/m^{2}s, x=0.9, T=33ºC)

Visualization and classification of flow regimes for mass flux from 40 to 150 kg/m^{2}s with flow direction right to left are shown in Figure 6. Data are drawn in three symbols that represent different flow patterns: Δ-slug/stratified-wavy, □-stratified-wavy, and ◊-annular. In this mass flux range, vapor slugs appear in a zone with relative low quality. As the vapor quality increases, so thus the frequency of vapor slugs. The length of liquid bridges between vapor slugs become smaller. As the quality increases to a certain range, liquid bridges break down and the liquid and vapor interface appears in the middle in a wavy form. The height of the waves reduces as the quality increases. When the mass flux is high, liquid is flowing along the entire tube wall with vapor in the core. The liquid film at the bottom of the tube is thicker than at upper part of the tube. When the quality equals to one, no liquid refrigerant should appear in the test section.

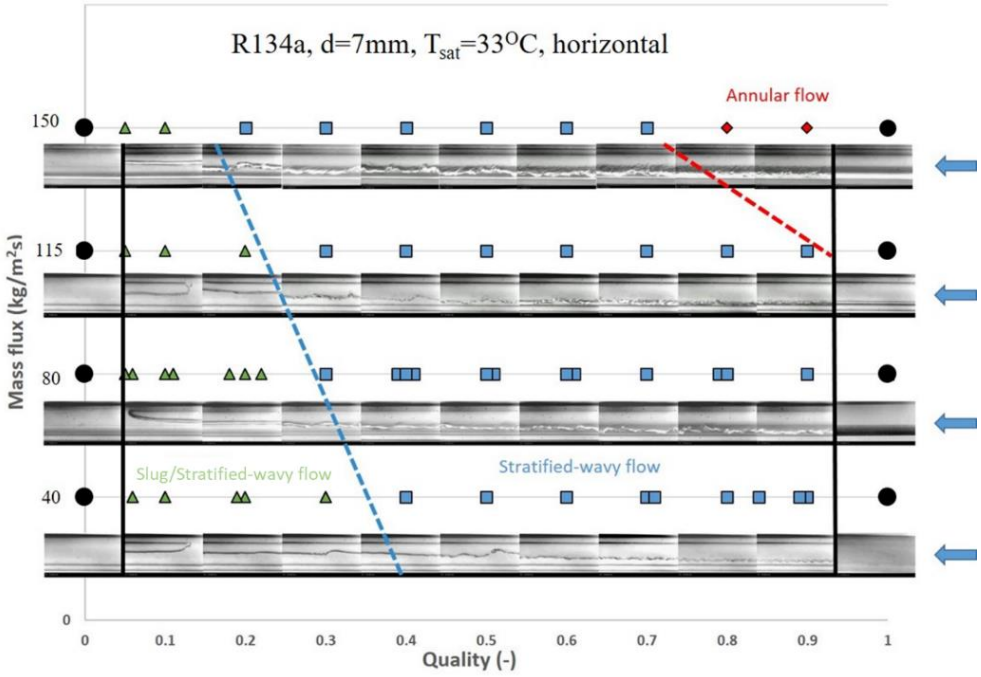

Figure 6 Visualization and classification of flow regimes for horizontal flow

Visualization and classification of flow regimes is shown in the modified Wojtan-Ursenbacher-Thome (Wojtan *et al.*, 2005) flow map (Figure 7). Wojtan-Ursenbacher-Thome (Wojtan *et al.*, 2005) flow map was developed for flow boiling in horizontal tubes. However, in this paper, refrigerant is first heated into superheat phase and then condensed into two-phase region. So, dryout and mist regimes will not appear. In addition, the measurements are performed in adiabatic conditions. Hence, dryout and mist regimes in the flow regime map by Wojtan et al. (Wojtan *et al.*, 2005) are omitted. They suggested only two major flow patterns in this mass flux range: slug/stratified-wavy and stratified-wavy flow, which is different from observed and described in this study: slug/stratified-wavy flow, stratified-wavy flow and annular flow. Some discrepancies are discussed as following:

1. When vapor quality is lower than the transition line between flow (x_{IA}), Wojtan et al. (Wojtan *et al.*, 2005) found slug flow and stratified-wavy flow coexist with the dynamic void fraction as defined in Wojtan *et al.* (2005) measurements. As the quality increases from 0 to x_{IA}, vapor slugs become longer and then liquid bridges breaks. The transition between slug/stratified-wavy and stratified-wavy flow in the visualization results of this study has some discrepancies to the transition line in the flow regime map. The flow regime map indicates higher vapor qualities as the transition line than the classification in this study.
2. The annular flow zone from the map (Wojtan *et al.*, 2005) should be extended. With the mass flux of 150 kg/m^{2}s, annular flows appear at the higher vapor quality zone. Hence, under adiabatic conditions, the transition line between annular flow and stratified flow in Wojtan et al. (Wojtan *et al.*, 2005) flow regime map should keep the slow decreasing trend at x=0.7 rather than increase dramatically when qualities is near unity.

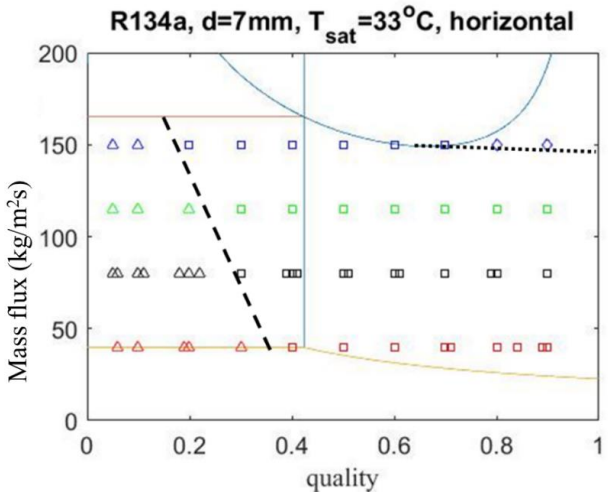

Figure 7 Classification of flow regimes for R134a in the modified Wojtan-Ursenbacher-Thome (Wojtan *et al.*, 2005) flow map (Δ-slug/ stratified-wavy flow, □-stratified-wavy flow, − transition lines from the flow map, -- transition line between slug stratified-wavy flow and stratified-wavy flow in this paper, ⋯ transition line between annular flow and stratified flow in this paper)

Figure 8 shows the comparison of some correlations that Woldesemayat and Ghajar (2007) recommended vs. our data at mass flux G=115 kg/m^{2}s. Results for other mass fluxes are similar and omitted due to the space limitation of this paper. Void fraction increases dramatically in low quality range (0<x<0.15). This is because liquid phase density is much greater than vapor phase density. Even low vapor quality in the test section requires relatively large vapor volume.

In this mass flux range, experimental data agree pretty well to the correlations of Woldesemayat and Ghajar (2007) and Rouhani I (Woldesemayat and Ghajar, 2007). The correlations of Armand (1959)-Massena (1960) predict higher void fraction than our experimental data. This correlation becomes closer to the data as mass flux increases. The homogeneous correlation predicts higher values than data in this paper. The homogeneous model predicts the upper limit of void fraction results.

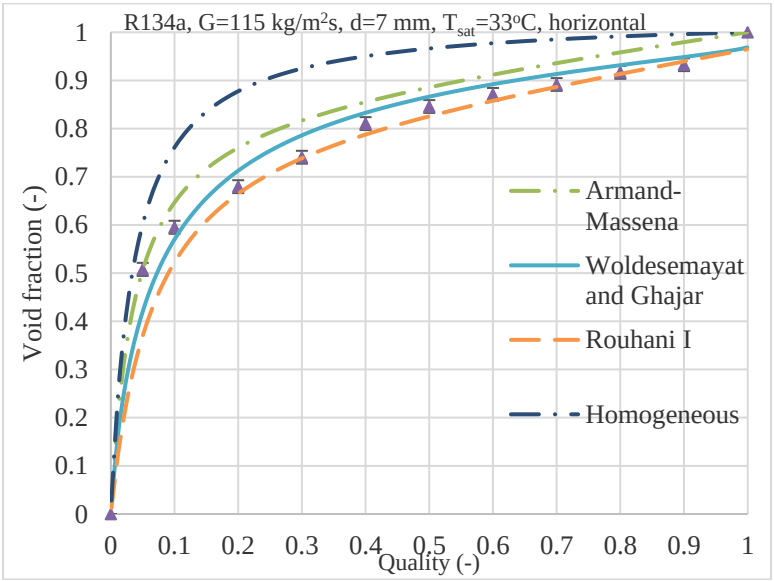

Figure 8 Experimental data are in good agreement with void fraction correlation Woldesemayat and Ghajar (2007) with exception for very high quality, in conditions explored G=115 kg/m^{2}s @ 33ºC, horizontal

This experiment is conducted in adiabatic condition. Hence, as vapor quality is approaching to unity, void fraction is supposed to approach to one asymptotically. However, correlations Woldesemayat and Ghajar (2007) and Rouhani I (Woldesemayat and Ghajar, 2007) do not show this trend, while homogeneous and Armand (1959)-Massena (1960) do. Two last predictions are not as good as the first two in mass flux range explored for R134a. In conclusion,

Woldesemayat and Ghajar (2007) and Rouhani I (Woldesemayat and Ghajar, 2007) correlations give reasonably good predictions for adiabatic horizontal flows with R134a and this mass flux range, with caution when using them around quality equals one.

3.2 Flow regimes and void fraction for vertical upward flow

For the flow upwards in vertical configuration, a high-speed camera is also used to capture flow patterns. Unlike in horizontal orientation, we observed slug, churn, and annular patterns. Criteria for each flow regime are listed below:

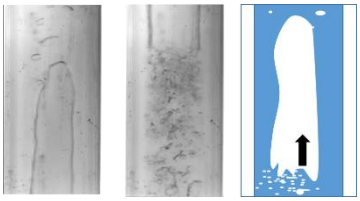

Figure 9 Slug flow (R134a, 80 kg/m^{2}s, x=0.1, T=33ºC)

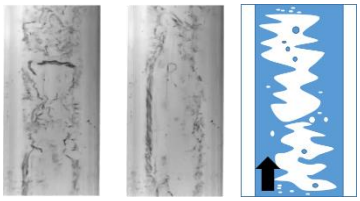

Figure 10 Churn flow (R134a, 80 kg/m^{2}s, x=0.5, T=33ºC)

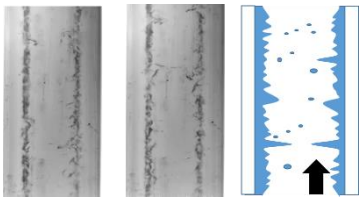

Figure 11 Annular flow (R134a, 115 kg/m^{2}s, x=0.9, T=33ºC)

Slug flow: vapor slugs appear periodically with liquid bridge in the middle. The slugs are in the middle of the tube and filling almost the entire cross section due to the direction of gravity is opposite of the flow.

Churn flow: the total effect combined of shear on interface, pressure gradient and gravity on a droplet is not constant upwards. This results in chaotic structure of the flow: liquid may go up and down intermittently though the mean velocity of the two-phase mixture points up. This flow pattern is highly agitated and the interface between liquid and vapor is hard to locate.

Annular flow: liquid flows along the wall of the tube with vapor in the central core. It is relatively more stable and less chaotic than churn flow though the interface between liquid and vapor core is wavy.

Visualization and classification of flow regimes is shown in Figure 12. Flow regimes presented are for mass flux ranging from 65 to 115kg/m^{2}s and temperature 33ºC. Data are shown in dots with three different symbols that represent different flow patterns: Δ-slug, □-churn, and ◊-annular flow. Due to the limitation of experimental instruments, vapor qualities lower than 0.05 cannot be obtained in steady state. Hence, bubbly flows which are supposed to be observed before slug flows are not captured by the high-speed camera in steady states. When the vapor quality is relatively low, vapor slugs and small bubbles periodically appear in the test section. As the quality increases, the flow pattern becomes more chaotic and the interface gets blurrier. It can be seen that even overall liquid flows up and then downwards for short time. When the vapor quality approaches to unity, the flow pattern becomes more stable. Vapor flows in the central core of the tube with liquid along the wall. As the vapor quality increases to one, no liquid appears in the test section.

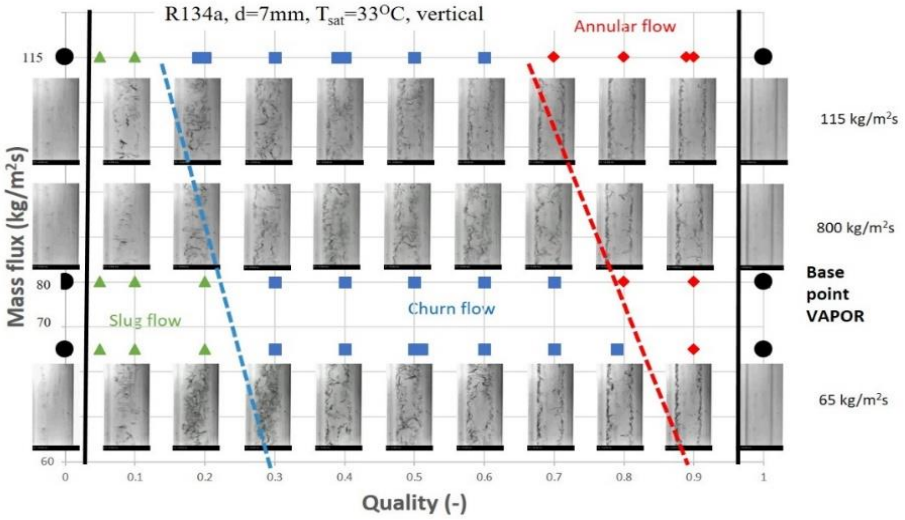

Figure 12 Visualization and classification of flow regimes for vertical flow

Figure 13 shows the void fraction at mass flux of G=65 kg/m^{2}s compared with several correlations: Rouhani I and

Rouhani II (Woldesemayat and Ghajar, 2007), Dix (1971) and Nicklin (1962). Results for other mass fluxes are similar and omitted for the sake of simplicity. For the upwards vertical configuration, the void fraction shows similar trend to horizontal configuration.

In this mass flux range, experimental data agrees pretty well to the Rouhani II (Woldesemayat and Ghajar, 2007) and Dix (1971), followed by Rouhani I (Woldesemayat and Ghajar, 2007). Nicklin (1962) correlation gives larger predictions than the experimental data in the low-vapor-quality range and smaller predictions in the high-quality-range. Homogeneous correlation also gives the largest prediction and no data is larger than its prediction.

Experiments in vertical upward flow configuration are also conducted in adiabatic conditions. As vapor quality is approaching one, void fraction is supposed to approaching to one asymptotically. However, no correlations studied in this section except homogeneous correlation show this trend. Hence, when utilizing Rouhani II (Woldesemayat and Ghajar, 2007), Dix (1971) and Rouhani I (Woldesemayat and Ghajar, 2007) correlations for adiabatic flow with R134a in this mass flux range to predict void fraction, special cautions should be applied when quality is near one. In conclusion, Rouhani II (Woldesemayat and Ghajar, 2007), Dix (1971) and Rouhani I (Woldesemayat and Ghajar, 2007) give relatively good predictions of void fraction for adiabatic vertical flow with R134a in this mass flux range.

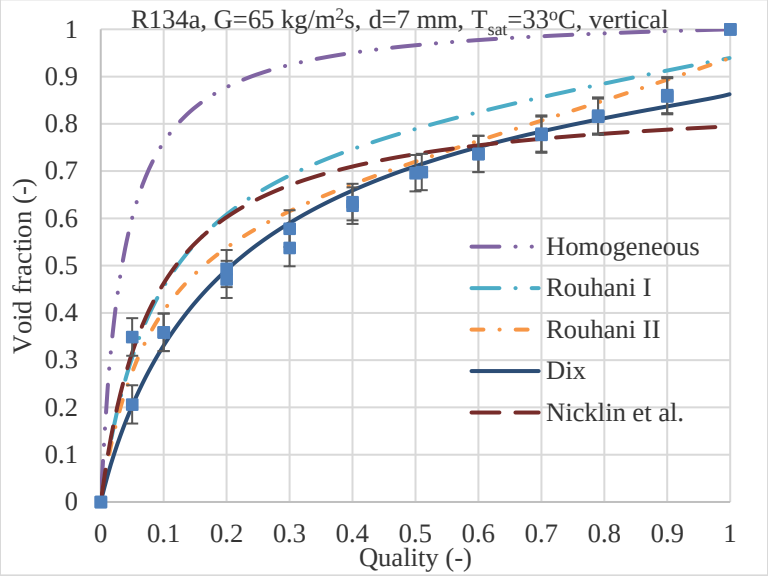

Figure 13 Experimental data are in good agreement with void fraction correlation Dix (1971) with exception for very high quality, in conditions explored G=65 kg/m^{2}s @ 33ºC, vertical

3.3 Influence of mass flux on void fraction

Figure 14 presents the trends of measured void fraction as mass flux increases for horizontal flows. The data shows that as mass flux increases, measured void fraction for a certain vapor quality will also increase. This can be explained that when mass flux increases, higher speed vapor may carry more liquid with it (the entrainment ratio is higher). The velocity difference between liquid and vapor phase reduces and they are acting more like two-phase mixture with same velocity (homogeneous flows). At the same quality, the ratio of vapor mass flow rate and liquid mass flow rate keeps constant. This results in the ratio of average area occupied by vapor to average area occupied by liquid becomes larger. Void fraction thus increases. Measured void fraction also increases as mass flux increases for vertical upward flows which is not shown.

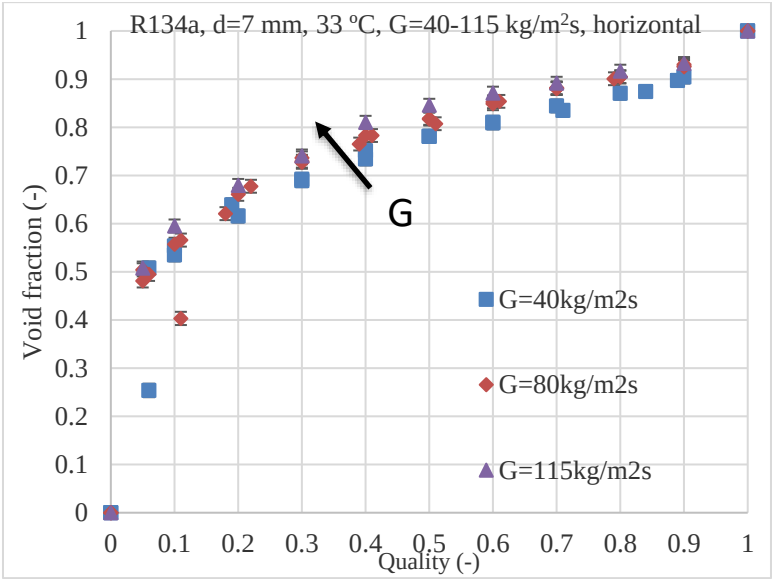

Figure 14 Void fraction increases as mass flux increases at the same quality @33 ºC, horizontal

Some correlations from categories of drift flux and general empirical show this trend while many in categories of slip ratio and $K\alpha_H$ categories not. Hence, when predicting void fraction with correlations for different mass flux, the former two categories are recommended. In this study, this phenomenon agrees to the predictions from Rouhani I (Woldesemayat and Ghajar, 2007) for horizontal flows and Dix (1971) for vertical flows.

3.4 Influence of tube orientation on void fraction

Figure 15 compares the measured void fraction results in horizontal flows and vertical flows at the same mass flux (G=80 kg/m^{2}s). Results for mass flux of G=115 kg/m^{2}s are similar and now shown here. In both mass flux conditions (80 kg/m^{2}s and 115 kg/m^{2}s), void fraction in vertical upward flows is lower than in horizontal orientation flows. This may be partially due to the slip ratio difference between the two tube orientations. In the upwards vertical flow, gravity will decrease liquid velocity more and enlarge velocity difference between liquid phase and vapor phase. This results in higher slip ratio and void fraction is lower.

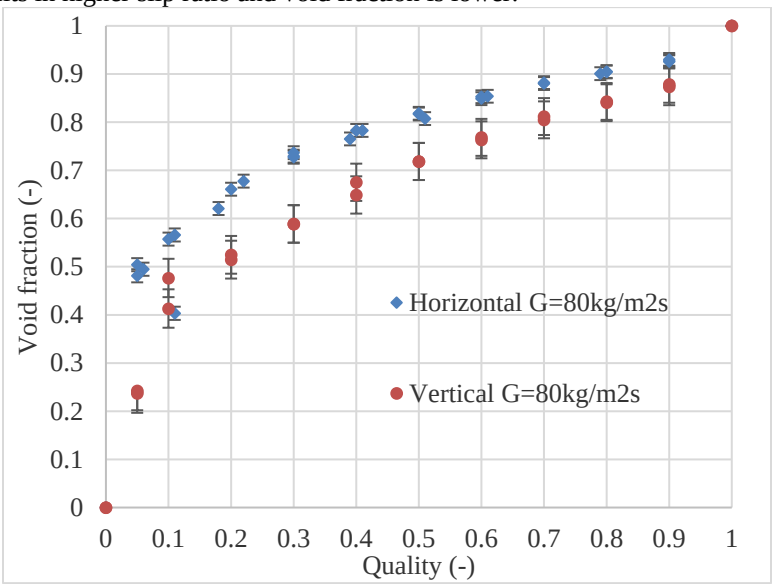

Figure 15 Void fraction is higher in horizontal than in vertical upward flow (G=80 kg/m^{2}s, 33 ºC)

4. CONCLUSIONS

- Flow regimes and void fraction in horizontal and vertical (at given location) round tubes with R134a in adiabatic conditions and low mass flux range are presented. In these conditions, three major flow patterns are observed in the test section for the horizontal flows: slug/stratified-wavy flow, stratified-wavy flow and annular flow. Based on the results, authors are proposing modification of the flow-pattern map by Wojtan *et al.* (2005) as presented with dashed lines in Figure 7.
- Three major flow patterns are observed for vertical upward flow: slug flow, churn flow and annular flow. The flow regime map in Figure 12 is proposed for vertical upward flow of R134a in conditions explored.
- For horizontal flows in this mass flux range, Woldesemayat and Ghajar (2007) and Woldesemayat and Ghajar version of Rouhani I (Woldesemayat and Ghajar, 2007) correlations give reasonably good predictions except for high quality (see Figure 8.). Woldesemayat and Ghajar version of Rouhani II (Woldesemayat and Ghajar, 2007) and Dix (1971), follows by Rouhani I (Woldesemayat and Ghajar, 2007) have good predictions for vertical upward flows (see Figure12.). As vapor quality is approaching to unity, void fraction is supposed to approach one asymptotically. However, the correlations mentioned above failed to show this trend. Be cautious when predicting void fraction for the vapor qualities close to one.
- Mass flux and tube orientation affect void fraction. Higher mass flux results higher void fraction. Void fraction in horizontal flow is higher than in vertical upward flow for the same conditions.
- Woldesemayat and Ghajar (2007) and Woldesemayat and Ghajar version of Rouhani I (Woldesemayat and Ghajar, 2007) correlations for horizontal flow and Woldesemayat and Ghajar version of Rouhani II (Woldesemayat and Ghajar, 2007) and Dix (1971) for vertical upward flows are recommended.

NOMENCLATURE

C_0	Distribution parameter	(–)
G	Mass flux	(kg/m^2s)
U_M	Two-phase mixture velocity	(m/s)
U_{SG}	Superficial vapor velocity	(m/s)
U_{SL}	Superficial liquid velocity	(m/s)
U_{GM}	Drift velocity	(m/s)
x	Vapor quality	(–)
α	Void fraction	(–)
ρ	Density	(kg/m^3)
σ	Surface tension	(N/m)

Subscript

H	Homogeneous
V	Vapor phase
L	Liquid phase
r	Refrigerant

REFERENCES

Armand, A. A. (1959). *Resistance during the movement of a two-phase system in horizontal pipes.*

Dix, G. E. (1971). *Vapor void fractions for forced convection with subcooled boiling at low flow rates*: University of California, Berkeley.

Godbole, P. V., Tang, C. C., & Ghajar, A. J. (2011). Comparison of void fraction correlations for different flow patterns in upward vertical two-phase flow. *Heat Transfer Engineering, 32*(10), 843-860.

Massena, W. (1960). *Steam-water Pressure Drop and Critical Discharge Flow-A Digital Computer Program*. Retrieved from

Nicklin, D. (1962). Two-phase flow in vertical tube. *Trans. Instn. Chem. Engrs., 40*, 61-68.

Wojtan, L., Ursenbacher, T., & Thome, J. R. (2005). Investigation of flow boiling in horizontal tubes: Part I—A new diabatic two-phase flow pattern map. *International Journal of Heat and Mass Transfer, 48*(14), 2955-2969. doi:https://doi.org/10.1016/j.ijheatmasstransfer.2004.12.012

Woldesemayat, M. A., & Ghajar, A. J. (2007). Comparison of void fraction correlations for different flow patterns in horizontal and upward inclined pipes. *International Journal of Multiphase Flow, 33*(4), 347-370. doi:https://doi.org/10.1016/j.ijmultiphaseflow.2006.09.004